

## Development and Characterization of a Radiation Scanning System for Small Organ Studies.

R. Pérez Sánchez, H. E. Bañados Pérez, L. L. Campos,  
Instituto de Pesquisas Energéticas e Nucleares, Travessa R 400, Cidade Universitária,  
São Paulo SP, Brasil (CEP: 05508-900)  
Poster No 47 Poster Session No. 07

revisado

OK

PRODUÇÃO TÉCNICO CIENTÍFICA  
DO IPEN  
DEVOLVER NO BALCÃO DE  
EMPÉSTIMO

### I. INTRODUCTION.

According to data from the Brazilian Society of Biology and Nuclear Medicine there are in Brazil about 150 laboratories offering services in the Nuclear Medicine area and 40% of them utilize linear scanner devices. This service is applied to a few tens of thousand of people per month, in average all over the country. There are about 73 types of clinical tests commonly indicated by Brazilian medical personnel in this category, and about 30% of them correspond to evaluation of thyroïdal function. The utilization of a linear scanning device is justified by lower operational cost and less time necessary to obtain images from small organs (like thyroid), when compared to a gamma camera.

Recent works in this area (8,9) indicate that using artificial intelligence techniques, specifically artificial neural networks, for processing medical images is a promising method, that allows automatically obtaining reliable results with a faster processing, when compared with the conventional processing. More over, optimizing scanner components, i.e., detection system, collimator, scanning system, digital image processing, device control and operation software, is an important factor in performing diagnostics with quality.

In a typical thyroïdal study a proper radiopharmaceutical that is accumulated in the thyroïd (12,13) is administered to the patient in order to obtain the image of the obtained radioisotope distribution. The scintillographic image obtained from such study allows to evaluate the organ's state, locate the exact position for surgery, etc. A scintillographic image from a small organ as thyroïd, allows to determine the gland's position, either normal or incorrect (ectopic gland). The gland's relative size might indicate diseases such as hyperthyroidism. It is also important to search for nodes: hot nodes, with activity higher than the normal cells and cool nodes, with less activity. In a few cases there have been observed nodes with the same activity that the normal tissue (16).

This work is aimed to develop and characterize a prototype scintillographic scanner device to be used in thyroïd and other small organs studies. It will be part of a system developed at IPEN for evaluation of the thyroïdal function with automatic analysis using artificial neural networks.

In this work we discuss the materials and methods utilized to develop and characterize a scintillographic scanner and the results obtained.

### II. MATERIALS AND METHODS

The scintillographic scanner is formed by the radiation detection system and the control and acquisition module, described in the next paragraphs.

**Radiation Detection System:** The radiation detection system is composed by a NaI(Tl) scintillator detector ( $\varnothing 76\text{mm} \times 25\text{mm}$ ) and a lead collimator that is located at the point of intersection of the scanner axes, controlled by a couple of step motors. The detection system presents an energy resolution of 12% for  $^{99\text{m}}\text{Tc}$  ( $E_{\gamma}=140,51\text{keV}$ ) photo-peak.

The lead collimator was designed to work with  $^{131}\text{I}$  and  $^{99\text{m}}\text{Tc}$ . Its 1cm thick walls attenuate the most energetic radiation of the  $^{131}\text{I}$  ( $E_{\gamma}=364,48\text{keV}$ ) as much as 10 times. The cylindrical channel with 1mm diameter allows to collimate the radiation with a good spatial resolution.

**Control and Acquisition Modules:** The control and acquisition modules are formed by a SYNCRO ICH\_XY controller and a NOVELEC SM512 multichannel analyzer.

The NOVELEC SM512 is a portable multichannel analyzer with a RS-232 serial link with a microcomputer with all its functions available in a fully programmable interface. It was configured to work with the radiation of  $^{99\text{m}}\text{Tc}$ . The ICH\_XY module is also linked to a microcomputer via RS-232 and its programmable logic allows to operate the scanner and to keep control over the detection system's position and state. A set of MS Visual Basic modules was developed to control and monitor both SM512 and ICH\_XY via standard serial ports.

All the modules were integrated in a unique software that allows to monitor all the required parameters

during the process of scanning until each image is obtained. This software takes account of some adjustments needed during acquisition, such as compensate for radioisotope decay during an acquisition period. A set of norms was observed to guarantee the software development process with reduced errors and according to specifications, as described in (15).

### III. SCANNER PERFORMANCE IN IMAGE ACQUISITION

The capabilities and performance of the scanning system for the tasks of obtaining images of the radiation distribution were tested using a set of simulators with different geometries. In all cases was used a safe amount of  $^{99m}\text{Tc}$  to create the active region. Figure 1 shows the image obtained from a point source with  $\varnothing=2\text{mm}$ .

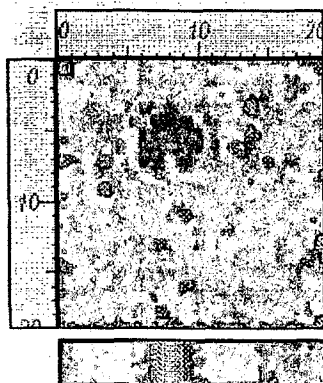


Figure 1: Image obtained from a point source of  $\varnothing=2\text{mm}$   $^{99m}\text{Tc}$ .

It was also used a set of thyroid phantoms formed with several pieces of filter paper saturated with a solution of  $^{99m}\text{Tc}$ . One of the obtained images is presented in Figure 2.

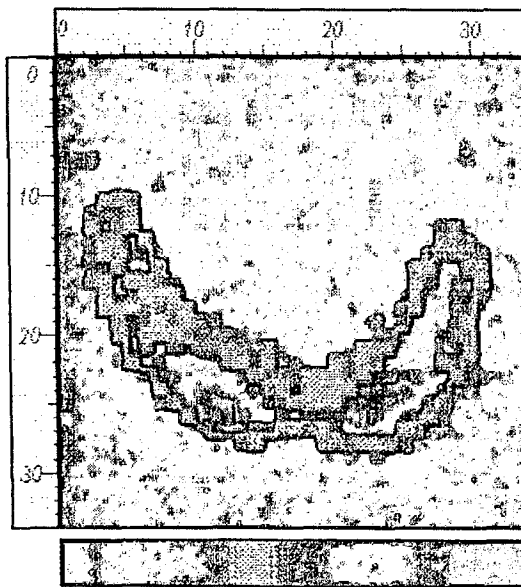


Figure 2: Image obtained from a thyroid simulator.

A wide discussion of the relevant characteristics in evaluating a scanner device from the point of view of plane image acquisition was presented in (14). The most important parameter for our work is that of the scanner's spatial resolution, i.e., the device capacity to detect two objects, situated one close to the other, as two different entities. An indicator of the spatial resolution is the full width at half-maximum (FWHM) of the point spread function (PSF) or the line spread function (LSF). While the LSF provides a complete description of resolution, it is

~~not in a very convenient form. A more convenient way is using the Modulation Transfer Function.~~

**Determination of the Modulation Transfer Function.** The Modulation Transfer Function (MTF) offers the most complete characterization of the spatial resolution of a scanning device, assuming the system response is linear. While the condition of linearity doesn't hold in this case, it is a good approximation and the MTF is very useful in evaluating the spatial resolution. The MTF is the spectrum of spatial frequencies that the device is able to reproduce (6, 14,17), and measures the contrast transfer from the object to the image as a function of the spatial frequency (object dimension).

The problem of comparing the performance of different types of devices has long proved a challenge. There have been devised a set of methods to objectively measure the spatial resolution of imaging devices (2,3,4). All of them require a careful measurement of the LSF in order to calculate the FWHM and then the MTF (14). For example, the standard NEMA (5) for evaluating the spatial resolution using the LSF requires acquiring a digital image from a linear source 1mm wide.

Meanwhile, other methods have been proposed to simplify this task with a cost in terms of loss of precision, but with the advantages of being quick and using simple equipment. One of this methods is based in computing the statistical moments in images of bar simulators with different step widths (1). Using the statistical moment method it can be computed an approximation to the actual MTF:

$$MTF(f) = \frac{[Peak(f) - Valley(f)] / 2}{[Peak(f) + Valley(f)] / 2} \quad (1)$$

where  $Peak(f)$  e  $Valley(f)$  are the maximum and minimum values of the sinusoidal frequency function  $f$ , assuming that the bar pattern in the image is a sinusoid.

Another simplified version for this method is the proposed in (10) with the modification of (11). This method uses the image obtained from an uniform simulator with linear edge in the scanner's vision field. This edge must be oriented in parallel to either the columns or the rows in the image. An approximated image of a thin linear source is obtained numerically differentiating the edge image, obtaining a LSF(x). The Fourier transform is applied to the LSF(x), to obtain the optic transformation function OTF(f). The MTF(f) is obtained as the modulus of OTF(f).

Both methods are in some way approximated, however, applied in combination they can evaluate more precisely from the point of view of image acquisition, with sufficient accuracy and low costs in terms of time and equipment. To apply the method of statistical moments were constructed simulators in the form of banner of different widths. The simulators were constructed with filter paper saturated with a solution of  $^{99m}\text{Tc}$ . Afterwards the piece of paper with the radioisotope was sealed with several layers of plastic to allow its use without any risk of contamination. Simulators with bars of different widths were prepared and measured: 1,5mm, 2mm, 3mm and 4mm. All the radiological security measures were observed. The images obtained are presented in Figures 3, 4, 5 and 6. Measurement time was 10s for each point.

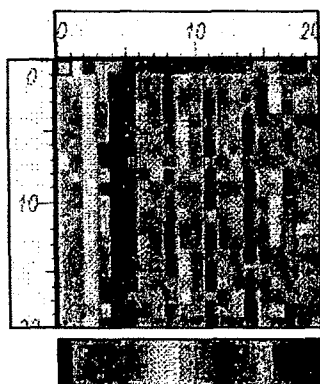


Figure 3: Image of bar simulator  $d = 1,5\text{mm}$ .

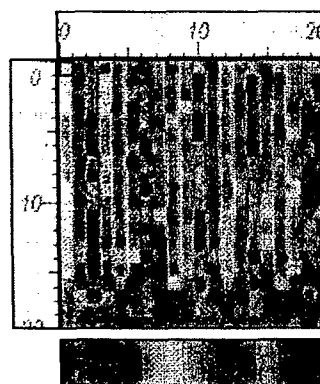
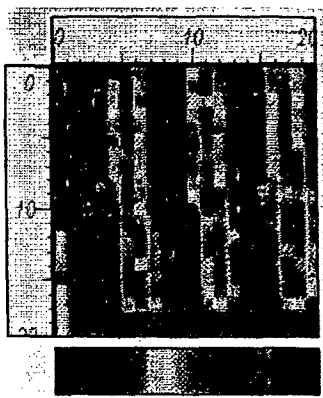
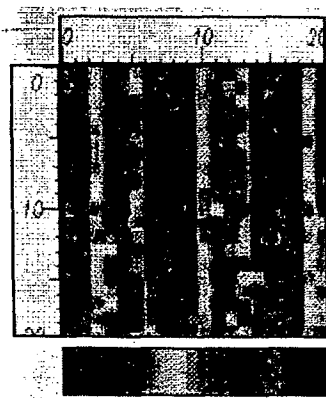


Figure 4: Image of bar simulator  $d = 2\text{mm}$ .

Figure 5: Image of bar simulator  $d = 3\text{mm}$ .Figure 6: Image of bar simulator  $d = 4\text{mm}$ .

Using a collimator with a thin channel guarantees a good spatial resolution (the bar simulator with  $d=1,5\text{mm}$  is reproduced adequately in Figure 3) at a cost of efficiency loss. This problem should be addressed with the development of a multichannel focal collimator.

To compute directly the  $\text{MTF}(f)$  it was obtained the image of an extended simulator with an edge in the center of the scanner's vision field. All the measurement conditions are the same. The image obtained is presented in Figure 7.

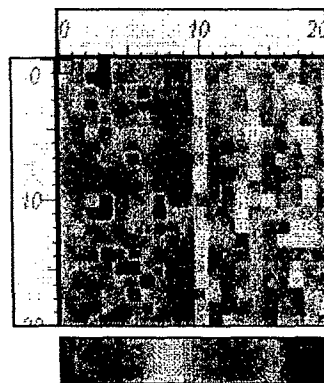


Figure 7: Image of an edge simulator.

The Fourier transform FT (zero padded to use a fast FT algorithm (7)) was applied to the  $\text{LSF}(x)$  resulted from the image's numerical derivative. The module of  $\text{OTF}(f)$  gives directly the  $\text{MTF}(f)$ . The  $\text{MTF}(f)$  calculated in such a way presents high values for frequencies above  $0,45\text{mm}^{-1}$ . This is a result of the effect of aliasing in calculating the FT, due to the sampling with finite intervals (step  $\Delta=1\text{mm}$ ) of noisy data. In fact, the random noise of nuclear data is treated as components of frequency above the critic frequency of Nyquist  $f_c=1/(2\Delta)$ , and the power corresponding to this interval of frequencies is transferred to the extremes of the interval  $[-f_c, f_c]$  of definition of the FT (7).

#### IV. RESULTS

The maximum detector position error in the scanning system was  $0,12\text{mm}$ .

In Figure 8 is showed the resulting  $\text{MTF}(f)$  obtained with both methods. The points obtained with the statistical moments method are in good agreement with values from  $\text{MTF}(f)$  (note that the continuous curve is a representation of an ideal  $\text{MTF}(f)$ , for illustration purposes).

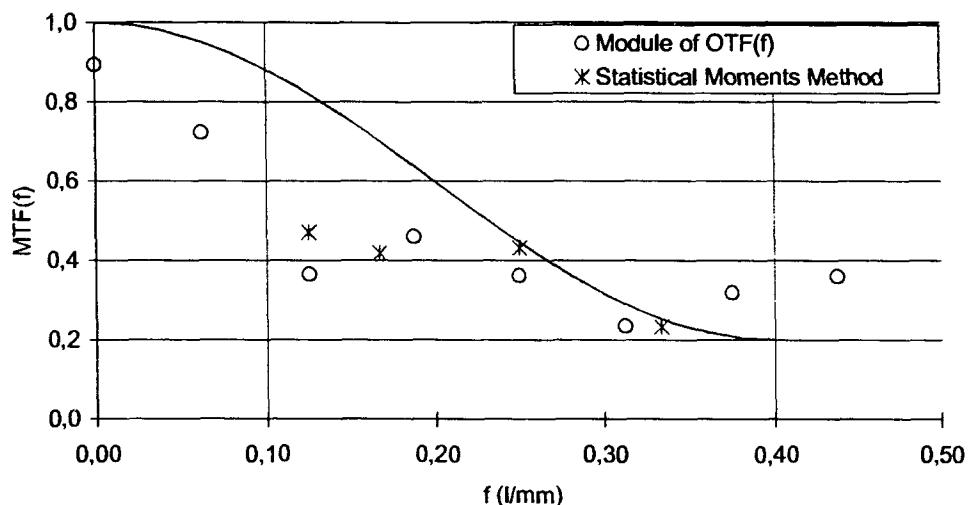


Figure 8. MTF( $f$ ) Calculated with both Statistical Moments and Fourier Transform of LSF( $x$ ).

These values for spatial resolution are comparable to those of gamma camera (1). The results of characterization of the scanning device represented in Figures 3-7 and in the graphic MTF( $f$ ) in Figure 8 allows to discriminate details of the order of 1,5mm. It means that the obtained images are adequate to the task of obtaining images of small organs such as thyroid.

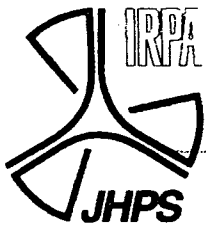
#### ACKNOWLEDGMENTS

This work was partially supported by a CAPES grant.

#### REFERENCES.

1. Hander T.A. et al., "Rapid objective measurement of gamma camera resolution using statistical moments", *Med. Phys.* 24(2), 327-334, February 1997.
2. J. Lancaster et al., "Practical Gamma Camera Quality Control with a Four-point Phantom", *J. Nucl. Med.*, 26, 300-307 (1985).
3. U. Raff et al., "Practicality of NEMA Performance Measurements for User-based Acceptance Testing and Routine Quality Assurance", *J. Nucl. Med.*, 25, 679-687 (1984).
4. B. Hasegawa et al., "Quality Control of Scintillation Cameras Using a Minicomputer", *J. Nucl. Med.*, 22, 1075-1080 (1981).
5. "Performance Measurements of Scintillation Cameras", Standards Publications No. NU1, Washington, DC: National Electric Manufacturers Associations, 1986.
6. "Detecteurs d'images en radiologie industrielle", Groupe Régional Dauphine-Savoie, Président J.F. Piquard, Grenoble, France, 1993.
7. "Numerical Recipes in FORTRAN", Second Edition, Press W.H. et al., Cambridge University Press.
8. Alirezaie J., Jernigan M.E., Nahmias C., "Neural Network-Based Segmentation of Magnetic Resonance Images of the Brain", *IEEE Trans. On Nucl. Sci.* V. 44, N. 2, April 1997.
9. Keller P. et al., "A Novel Approach to Modeling and Diagnosing the Cardiovascular System", Proceedings of the World Congress on Neural Networks (WCNN'95) in Washington, DC, USA, from 17-21 July 1995.
10. Fujita H. et al., "A simple method for determining the modulation transfer function in digital radiography", *IEEE Trans. Med. Imag.* MI-11, 34-39 (1992).
11. Yu T. et al., "Scintillating fiber optic screens: A comparison of MTF, light conversion efficiency, and emission angle with Gd<sub>2</sub>O<sub>2</sub>S:Tb screens", *Med. Phys.* 24 (2), pp. 279-285, February 1997.
12. Klain M. et al., "Tc-99m tetrofosmin imaging in thyroid diseases: comparison with Tc-99m-pertechnetate, thallium-201 and Tc-99m-methoxyisobutylisonitrile scans", *European Journal of Nuclear Medicine*, v. 23, n. 12, pp. 1568-1574, December 1996.

13. ~~Jaap Bonjer, H. et al., "Intraoperative Nuclear Guidance in Benign Hyperparathyroidism and Parathyroid Cancer", European Journal of Nuclear Medicine, v. 24, n. 3, pp. 246-251, March 1997.~~
14. Murphy P.H., J., "Acceptance Testing and Quality Control of Gamma Cameras, Including SPECT", Nucl. Med., v. 28, N. 7, pp. 1221 - 1227, July 1987.
15. Rosen I. I., "Writing Software for the Clinic", Med. Phys. 25 (3) pp. 301-309, March 1998.
16. "A Textbook of Radiology and Imaging", ed. Sutton D., 4<sup>th</sup> Ed. v. 2, Churchill Livingstone, New York, 1987.
17. "Radionuclide Imaging Techniques", Sharp P.F. et al., Academic Press, New York, 1985.

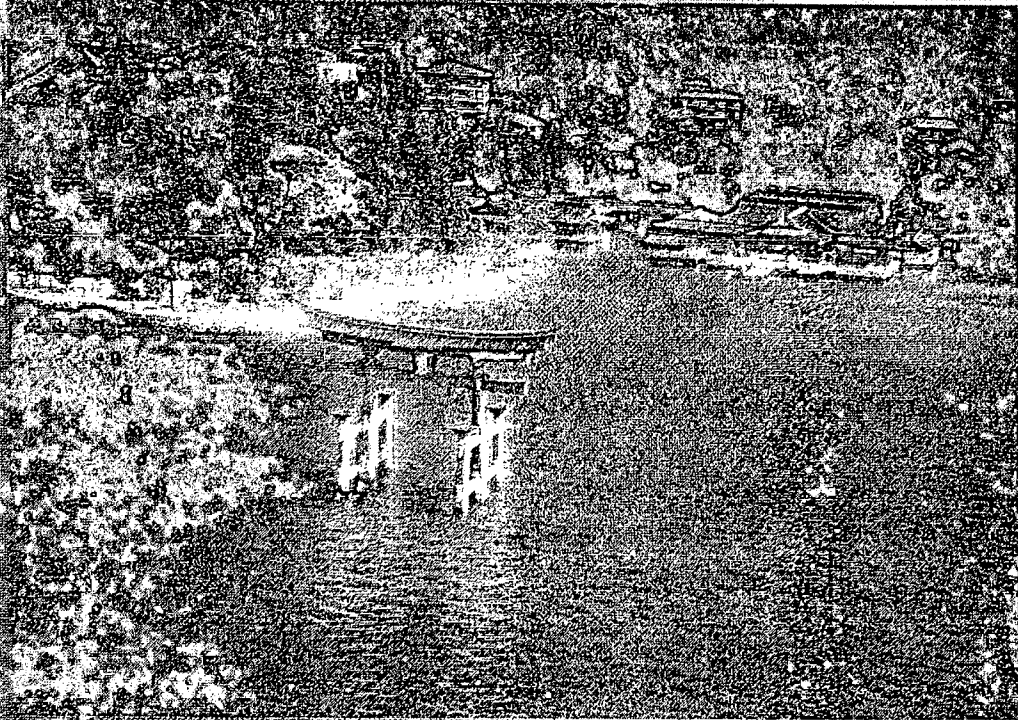


Postals

# IRPA-10

10th International Congress of  
The International Radiation Protection Association

*"Harmonization of Radiation,  
Human Life and the Ecosystem"*



## Proceedings

**International Conference  
Center Hiroshima  
May 14-19, 2000  
Hiroshima, Japan**